Feature article

Esterification of cetyl alcohol with palmitic acid over WO$_3$/Zr-SBA-15 and Zr-SBA-15 catalysts

Vahide Nuran Mutlu, Selahattin Yilmaz[*]

İzmir Institute of Technology, Chemical Engineering Department, Gülbahçe Kampüs, Urla İzmir, Turkey

ABSTRACT

Tungsten loaded and Zr incorporated SBA-15 catalysts (WO$_3$/Zr-SBA-15 and Zr-SBA-15) were developed for esterification of cetyl alcohol and palmitic acid. The influence of the Zr content, tungsten loading amount, calcination temperature, feed composition and catalyst amount has been studied. Higher tungsten loading decreased the acidity due to formation of WO$_3$ crystals whereas calcination temperature enhanced the acidity by favoring the dispersion of WO$_x$ species. Activities of the catalyst changed depending on their amount of Brønsted sites and total number of acid sites. Zr-SBA-15 catalyst which had the highest amount of Brønsted acid sites gave maximum cetyl palmitate yield (63.1%). This catalyst retained its activity up to 3 reuse cycles without significant loss of activity.

© 2016 Elsevier B.V. All rights reserved.

1. Introduction

Esters of fatty acids are used in many different areas, such as oiling agents and emulsifiers in food industry, personal care emollients surfactants and base materials for perfumes in cosmetic industry, solvents, lubricants for plastics, paint and ink additives. Among the different fatty acid esters, cetyl esters are commonly applied in cosmetic industry. Cetyl palmitate, cetyl stearate, myristyl myristate, and myristyl stearate are different types of cetyl esters. In the present study cetyl palmitate was produced by esterification of cetyl alcohol and palmitic acid through the reaction given below (Scheme 1).

Fatty acid esters are synthesized by esterification of fatty acids and alcohols in the presence of an acid catalyst and the reaction mechanism is called Fischer esterification. Fischer esterification reaction proceeds by nucleophilic attack of the alcohol on the protonated carbonyl group of the carboxylic acid to form a tetrahedral intermediate as shown in Scheme 2. Collapse of the intermediate regenerates the carbonyl group and produces the ester and water. Conventionally mineral acids such as concentrated sulfuric acid and hydrochloric acid are used as catalysts. These catalysts cause problems such as environmental hazards, difficulty in catalyst recovery and waste control, high susceptibility to water, requirement of a

large amount of catalyst and feedstock. Therefore, it is required to develop active, reusable and environmentally friendly heterogeneous catalysts.

Recent studies on heterogeneous catalysts for esterification reactions include zeolites [1,2], acidic resins [3,4], sulfated zirconia [5,6], tungstated zirconia [7–9] and heteropoly acids [10,11]. However, the success of the catalysis was limited to esters less than C$_{10}$ in either carboxylic acids or alcohols [12]. Sakthivel et al. studied esterification of different fatty acids and fatty alcohols over MCM-41 supported tungstophosphoric acid catalysts under supercritical conditions and reported high ester yields. However, catalyst leaching was observed [13]. Mantri et al. tested supported and unsupported multivalent metal salt hydrates for the esterification of long chain fatty acids and fatty alcohols. ZrO^{2+} was found to be an active metal cation for the esterification reaction with some other metals like Ga^{3+} and In^{3+}. Moreover, mesitylene was reported as a promising solvent with a yield of 89.3% at its boiling temperature (162 °C) in the same study among different solvents including benzene, toluene, m-xylene, diethylbenzene and tetralin [12].

Tungsten oxide based catalysts have been reported as active, thermally stable and promising catalysts for acid catalyzed reactions such as hydrocarbon isomerization [14–16], oxidation [17], acetylation [18] etherification and alkylation [19]. Ramu et al. studied esterification of palmitic acid with methanol over WO$_3$-ZrO$_2$ catalysts prepared by impregnation and co-precipitation methods and obtained fatty acid conversions up to 95% [7]. Park et al. compared WO$_3$-ZrO$_2$, sulfated ZrO$_2$ and Amberlyst-15 for conversion of
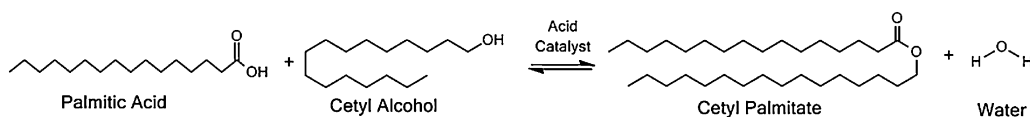
Scheme 1. Cetyl alcohol esterification with palmitic acid.

used vegetable oils to fatty acid methyl esters, and WO_3-ZrO_2 gave the highest conversion (93%) and no leaching of WO_3 was observed in the esterification reaction [8]. This was attributed to the strong interactions between WO_3 and ZrO_2 and high acidity of the catalysts. Despite their high activity and stability, WO_3-ZrO_2 catalysts have the disadvantage of small surface area and non-uniform pore size which may limit their activity for catalyzing the esterification of long chain fatty acids and fatty alcohols.

Mesoporous silicas were declared as promising catalyst supports in different studies [13,20,21]. Among different mesoporous silica materials SBA-15 was chosen for this study because of its high surface area and much thicker walls and consequently higher hydrothermal stability than MCM-41 [22,23]. To improve the surface acidity and broaden the applications, different metal ions have been incorporated into SBA-15 [24–27]. Garg et al. synthesized SBA-15 containing various amount (10–50 wt%) of highly dispersed ZrO_2 by urea hydrolysis method and tested these catalysts in esterification of cyclohexanol with acetic acid and cumene cracking. It was observed that, Zr doping did not destroy the hexagonal structure of SBA-15. As the ZrO_2 amount increased the total acidity and Brønsted acidity of the catalysts increased whereas the Lewis acidity decreased [28]. Biswas et al. prepared Zr-SBA-15 by chemical grafting (post synthesis) and direct hydrothermal synthesis. Zr-SBA-15 with higher surface area was obtained by direct hydrothermal synthesis. It was also reported that Zr loading improved the acidity of the catalyst [29]. Gracia et al. also investigated the hydrothermal synthesis of Zr-SBA-15. They synthesized well-structured Zr-SBA-15 mesoporous materials with high surface areas and narrow pore size distributions, containing both Lewis and Brønsted acid sites [30].

The effect of tungsten loading on Zr-SBA-15 was studied by Zhang et al. for the benzoylation of anisole. A series of strong acids WO_3/Zr-SBA-15 were prepared and the materials retained their mesoporous structure after WO_3 loading. The catalysts possessed both Lewis and Brønsted acid sites and exhibited considerably high activity for the benzoylation of anisole [31].

The studies about the esterification of long chain fatty acids and alcohols in the literature investigated the reaction parameters such

as reaction temperature, solvent type, and reactant ratio, while the effects of the catalyst preparation methods on the acidity and surface properties of the catalysts and on the yield of the esters were not examined in detail [12,13,32,33].

In the present work, the use of Zr incorporated SBA-15 (Zr-SBA-15) and tungsten oxide impregnated WO_3/Zr-SBA-15 mesoporous acidic catalysts in the esterification of cetyl alcohol by palmitic acid was reported for the first time. Effects of zirconia and tungsten contents, calcination temperature on the catalyst properties, activity and ester yield were examined. Different catalyst amounts and feed compositions were also studied.

2. Experimental

2.1. Catalysts preparation

Zr incorporated SBA-15 catalysts were prepared according to the method published by Zhang et al. with two different Zr molar amounts of $0.017P123:Si:0.08Zr:220H_2O$ and $0.017P123:Si:0.1Zr:220H_2O$). The catalysts were named as Zr-SBA15-08 and Zr-SBA15-10, respectively. $ZrOCl_2 \cdot 8H_2O$ was used as Zr precursor and tetraethyl orthosilicate (TEOS) was used as silica source. The synthesis was carried out with the preparation of a clear aqueous micelle solution of amphiphilic triblock copolymer P123. Then, $ZrOCl_2 \cdot 8H_2O$ solution with determined concentration and tetraethyl orthosilicate (TEOS) was added into the micelle solution and stirred at 37 °C for 24 h. Afterwards, the gel was placed in an autoclave and heated to 90 °C for another 24 h without stirring. The solid product was recovered by centrifuge, washed with deionized water and dried overnight at ambient conditions. The dried Zr-SBA-15 was calcined at 800 °C for 4 h in air flow.

Tungsten was loaded on to Zr-SBA-15 (15 wt% and 20 wt%) by incipient wetness impregnation from aqueous ammonium metatungstate solutions. The catalysts were kept in an ultrasonic bath in order to improve WO_3 dispersion over Zr-SBA-15 supports. After filtration, the product was dried at 110 °C for 12 h, and then the powder obtained was heated to calcination temperature with a heating rate of 2 °C/min. The catalysts were calcined at 700 °C and
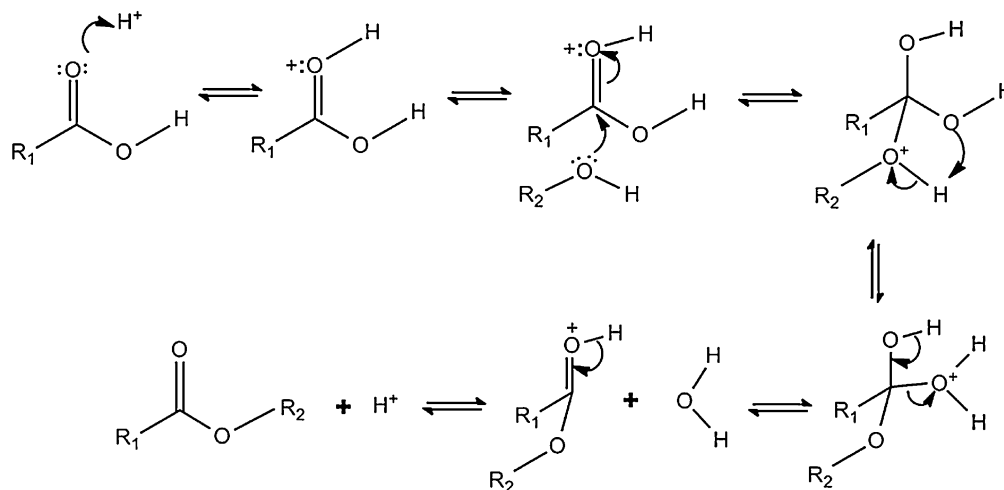
Scheme 2. Fischer esterification mechanism.

800 °C for 3 h and named as follows. For example, catalyst prepared with initial 0.08 mol of Zr, loaded 15% WO$_3$ and calcined at 700 °C was referred to as WZSBA08-15-7.

2.2. Characterization

Surface properties of catalysts were analyzed by nitrogen adsorption-desorption using Micromeritics ASAP 2010. N$_2$ adsorption was performed at 77 K following the degas step at 200 °C for 2 h. Specific surface areas were calculated by the BET method (S$_{BET}$).

Structural analysis of the catalysts were performed by X-ray diffraction and Raman spectra. The XRD patterns were obtained by Philips X'Pert diffractometer with CuKα radiation. The scattering angle 2θ was varied from 5 to 80, with a step length of 0.02. Raman spectra of the catalysts was obtained by an Argon laser at the excitation wavelength of 488 nm. The resolution was 4 cm^{-1}.

The framework vibration of synthesized Zr-SBA-15 and WO$_3$/Zr-SBA-15 catalysts were examined by FTIR spectroscopy. KBr pellet technique was employed to obtain infrared spectra of the samples at room temperature. The pellets were prepared with a sample amount of 3 wt%. The spectra was retrieved in the wavenumber range of 400–2000 cm^{-1} with a resolution of 4 cm^{-1} by an infrared spectrometer type Schimadzu FTIR 8400S.

NH$_3$-TPD method was applied to determine acid site distribution and quantify acidity of the catalysts using Micromeritics AutoChem II Chemisorption Analyzer. In a typical analysis, the powder was heated to 400 °C with a heating rate of 5 °C/min and kept at 400 °C for 30 min under 70 ml/min He gas flow. After cooling to 60 °C with a rate of 5 °C/min and reducing He flow to 30 ml/min, it was subjected to NH$_3$-He flow at the rate of 30 ml/min for 30 min. This was followed by degassing step at 60 °C under He flow of 70 ml/min for 2 h in order to remove the physically adsorbed NH$_3$. TCD signals were taken as the sample was heated to 700 °C with a rate of 10 °C/min.

Brønsted and Lewis acidity characteristics of the catalysts were determined by IR spectroscopy using pyridine adsorption/desorption method. For the analysis, the samples were kept at 300 °C under vacuum (2×10^{-2} mm Hg) for 2 h. Pyridine adsorption was performed at 150 °C for 30 min. Then, the sample was kept at 120 °C for 2 h under N$_2$ flow of 30 ml/min for desorption of the physisorbed pyridine. Shimadzu FTIR 8400S model Fourier Transformed Infrared Spectrometer was used to carry out the IR analysis of sample pellets between 400 and 4000 cm^{-1}. The sample pellets were prepared using KBr. The concentration of the pyridine adsorbed catalyst in the KBr pellet was 3 wt%.

Elemental compositions of the catalysts before and after their use in the reaction were analyzed by XRF method. The analysis was performed with powder method by using Spectro IQ II instrument and CuKα radiation.

2.3. Catalytic activity

Cetyl alcohol (CA) and palmitic acid (PA) esterification reactions were performed under N$_2$ atmosphere in a four necked round bottom flask (250 ml) equipped with a Teflon coated magnetic stirring bar with a stirring rate of 520 rpm and a Dean Stark apparatus surmounted with a reflux condenser. In a typical experiment, 160 mg of catalyst was added into 25 ml of mesitylene and heated up to reaction temperature of 162 °C. An equimolar solution of palmitic acid and cetyl alcohol (6 mmol) in 15 ml of mesitylene at room temperature was added into the reactor. All the reactions were carried out for a reaction time of 6 h. In a preliminary set of experiments (Table 1) it was found that the reaction was not controlled by external diffusion at 520 rpm. Samples taken at regular intervals were analyzed by Agilent 6890 gas chromatography using Ultra 1 (25 m × 0.3 mm) capillary column equipped with FID. The injector

Table 1
Influence of stirring rate on the initial disappearance rate and conversion of cetyl alcohol and the yield of cetyl palmitate over Zr-SBA15-08.

Stirring rate (rpm)	$r_{0\times} 10^5$ (mol min^{-1} g^{-1})	Conversion (%)[a]	Yield (%)[a]
520	9.23	64.3	63.1
750	9.59	64.6	63.8

[a] At 6 h reaction time.

temperature was 280 °C and the detector temperature was 320 °C. The GC oven temperature was changed from 50 °C at 12 °C/min to 300 °C where it was kept for 35 min. Helium was used as the carrier gas at a flow rate of 37.3 ml/min The split ratio was 24.9:1. Conversion of cetyl alcohol (CA), yield of cetyl palmitate (CP) and the selectivity to CP were defined as below.

$$Conversion(\%) = \frac{(CA_{in} - CA_{out})}{CA_{in}} \times 100$$

$$Yield(\%) = \frac{CP_{out}}{CA_{in}} \times 100$$

$$Selectivity\ to\ CP(\%) = \frac{CP_{out}}{(CA_{in} - CA_{out})} \times 100$$

The reusability of the three catalysts providing the most ester yields were tested. For this, the used catalysts were separated from the reaction mixture by filtration and washed twice with mesitylene and methanol. Subsequently, the catalysts were dried overnight at ambient conditions and heat treated at 550 °C for 6 h. Then, they were tested in the reaction again.

3. Results and discussion

3.1. Catalyst characterization

3.1.1. Phase characterization and surface properties

The XRD analysis showed that the hexagonal structure of SBA-15 was preserved after Zr incorporation (results not reported). When the spectra of Zr-SBA15-08 and Zr-SBA15-10 were compared, it was observed that the intensities of the characteristic peaks decreased with increasing Zr amount. This might be attributed to the decay in the orderliness of the structure because of the presence of more Zr in the mesoporous channels. Fig. 1 displays the XRD patterns of WO$_3$/Zr-SBA-15 catalysts. The labelled diffraction peaks are related to WO$_3$ crystals. The intensities of these peaks increased with the loading amount and calcination at the lower temperature. This indicated that the higher calcination temperature favored well dispersion of WO$_3$ on Zr-SBA-15 support by transforming the WO$_3$ crystals into smaller particles. Similar observations are also reported in literature [31].

Additionally, Raman spectroscopy was applied as a sensitive technique for detection of very small WO$_3$ crystallites. The Raman spectra of the catalysts is given in Fig. 2. WO$_3$/Zr-SBA-15 catalysts showed a broad band at 976 cm^{-1} assigned to W=O stretching in hydrated interconnecting polyoxotungstate clusters, and it is the characteristic sign for monolayer WO$_3$ dispersion. These WOx species generally have been related with the formation of strong Brønsted acid sites under reducing environment. Other bands observed in the Raman spectra of all catalysts at 807, 716, 324 and 275 cm^{-1} indicate the existence of WO$_3$ crystals. The bands at 807 and 716 cm^{-1} represents the stretching mode, while the bands at 324 and 275 cm^{-1} are attributed to the W=O bending mode and W—O—W deformation mode, respectively. Moreover, as the WO$_3$ loading amount increases, the areas of all these bands increase, showing that both the crystalline and highly dispersed
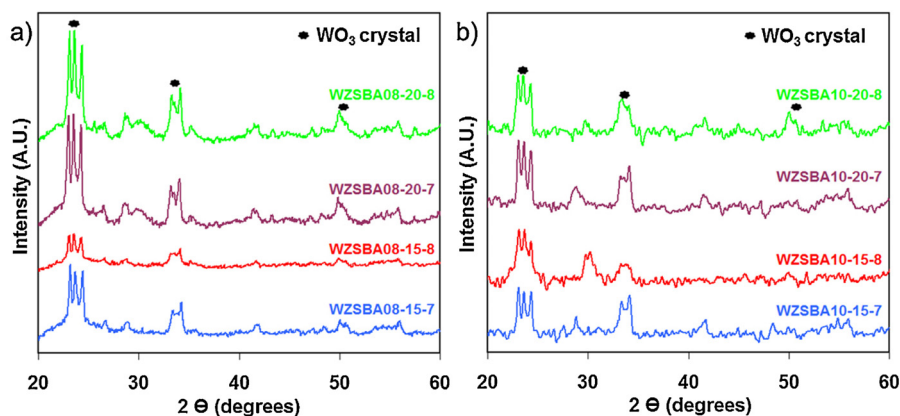
Fig. 1. XRD patterns of the catalysts prepared (a) WO$_3$/Zr-SBA15-08 and (b) WO$_3$/Zr-SBA15-10.

WO$_3$ increase simultaneously. When the effect of calcination temperature was considered, the band at 976 cm^{-1} indicating the monolayer dispersion of WO$_3$ enhanced with increasing calcination temperature. Thus, the calcination temperature affected the character of the acid sites of the catalysts, since these WOx clusters are associated with the Brønsted acid sites. It can be deduced from the results of Raman and XRD that the surface W will change from highly dispersed state into a coexistence of dispersed and crystalline WO$_3$ as the loading amount increases. The interaction between the support and WO$_3$ changed with calcination temperature and the monolayer dispersing appears as the calcination temperature increased.

All the catalysts exhibited a type-IV adsorption isotherm with a hysteresis loop, which correspond to a hexagonal pore system (results not reported) [28,29]. The textural properties of the catalysts are given in Table 2. The catalysts were mesoporous. Their surface areas and pore sizes decreased by WO$_3$ loading and calcination temperature. This was attributed to the presence of WO$_3$ clusters in the pores and on the external surface.

3.1.2. Acidic properties

The nature of acid sites of the catalysts was determined by FT-IR spectra of pyridine adsorbed catalyst samples as shown Fig. 3. The peaks at 1445 cm^{-1} indicate the pyridine coordination on Lewis acid sites, while the peaks at 1540 cm^{-1} are assigned to the pyridinium ion bonding to Brønsted acid sites and the peaks at 1495 cm^{-1} are related with both Lewis and Brønsted acid sites. To compare the concentrations of Lewis and Brønsted acid sites of the catalysts, the areas under the bands at 1445 cm^{-1} and 1540 cm^{-1} were related to Lewis and Brønsted acid site concentrations respectively [34]. The results indicated that tungsten loading decreased

Lewis and Brønsted acid sites. However, as the tungsten loading increased from 15 wt% to 20 wt%, the number of Lewis acid sites of the catalysts increased, while B/L ratio decreased (Table 2). Calcination temperature enhanced both Lewis and Brønsted acid sites. This was attributed to the increase in crystalline and highly dispersed WO$_3$ as observed by XRD and Raman analysis. WO$_3$ crystals led to Lewis acid while dispersed WOx sites, clusters are associated with the Brønsted acid sites [35]. Thus, in the FT-IR spectra the area of the peaks indicating the Brønsted acid sites increased with calcination temperature, whereas the area of the peaks assigned to Lewis acid sites increased with tungsten loading.

The acidities of the catalysts obtained by NH$_3$-TPD are given in Fig. 4. All the catalysts had broad acidity peaks between 200 °C and 400 °C indicating that the catalysts had moderate acidity. From the area under the TPD profiles of the catalysts, total acidity of the catalysts were determined and given in Table 2. It was found that Zr-SBA15-08, Zr-SBA15-10 and WZSBA08-15-8 were the most acidic catalysts.

3.2. Esterification of cetyl alcohol and palmitic acid

Cetyl palmitate was the only major product obtained over all the catalysts. The selectivities to cetyl palmitate were higher than 98% which showed that selectivity was independent of the catalyst properties.

3.2.1. Influence of Zr and W loading and calcination temperature

The results given in Fig. 5 display the conversion of cetyl alcohol over the catalysts. Cetyl alcohol amount decreased differently with reaction time depending on the catalyst. Zr-SBA15-08, ZrSBA15-10 and WZSBA15-08-8 provided higher cetyl alcohol conversions and
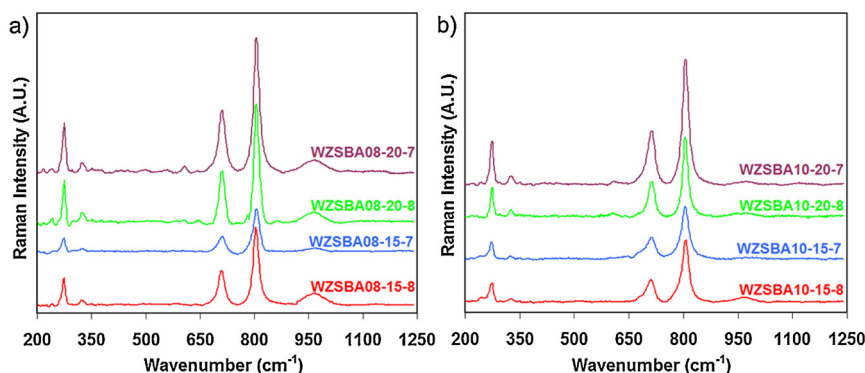

Fig. 2. Raman spectra of the catalysts prepared (a) WO$_3$/Zr-SBA15-08 and (b) WO$_3$/Zr-SBA15-10.

Table 2
Textural properties and total acidities of the catalysts prepared.

Catalysts	BJH d_P (Å)	S_{BET} (m²/g)	Acidity (mmol NH_3/g catalyst)	B/L[a]	Zr content (wt %)	W content (wt %)
Zr–SBA15-08	42.4	600.3	1.122	1.39	6.0	–
WZSBA08-15-7	35.6	323.4	0.718	1.22	11	7.7
WZSBA08-15-8	37.6	320.5	1.43	1.29	8.3	4.9
WZSBA08-20-7	37.3	299.8	0.684	0.71	12.5	10.1
WZSBA08-20-8	25.9	230.0	1.000	1.05	8.6	7.0
Zr–SBA15-10	34.4	548.6	1.069	1.37	8.0	–
WZSBA10-15-7	37.6	318.7	0.713	1.21	13.2	7.5
WZSBA10-15-8	37.6	318.7	0.996	1.26	10.6	4.6
WZSBA10-20-7	25.1	180.4	0.679	0.72	14.1	9.8
WZSBA10-20-8	33.6	148.3	0.966	0.90	12.7	8.5

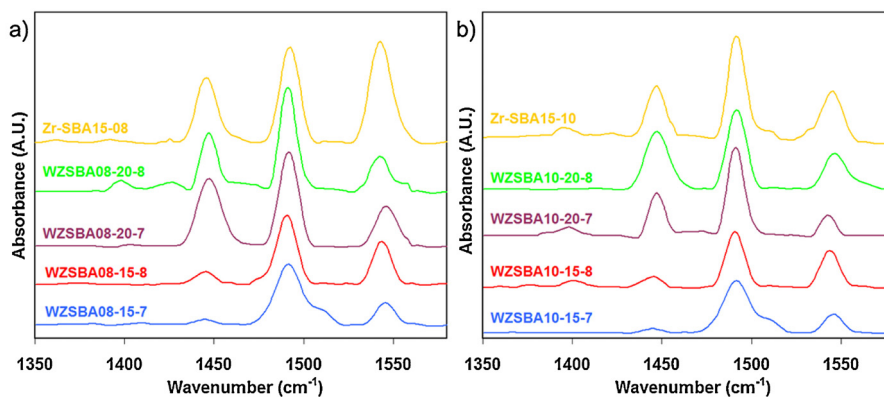[a] B/L defined as the ratio of the areas under the peaks at 1540 cm⁻¹ to 1445 cm⁻¹.

Fig. 3. FTIR spectra of pyridine adsorption on (a) Zr–SBA15-08 and (b) Zr–SBA15-10 based catalysts.

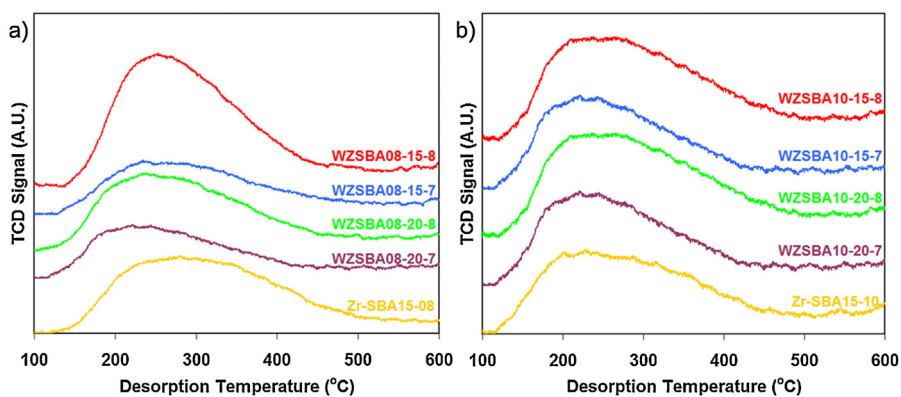**Fig. 4.** NH_3-TPD of the catalysts prepared, (a) Zr–SBA15-08 and (b) Zr–SBA15-10 based catalysts.
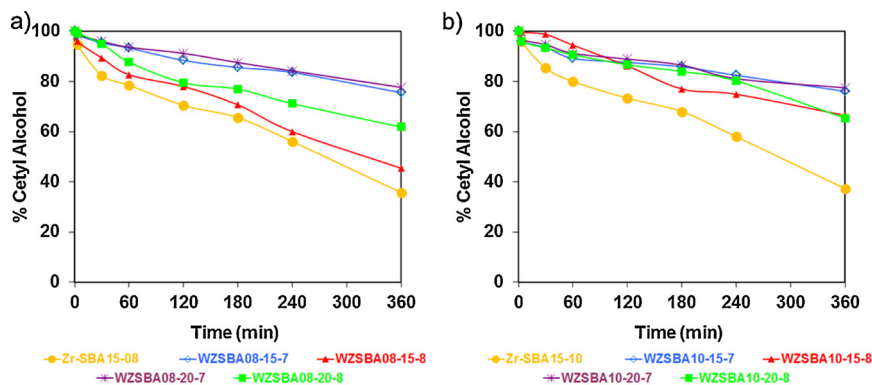

Fig. 5. Catalytic results for the esterification of cetyl alcohol and palmitic acid over (a) Zr–SBA15-08 and (b) Zr–SBA15-10 based catalysts.

Table 3
Initial rate of disappearance and conversion of cetyl alcohol and yield of cetyl palmitate over different catalysts at 162 °C after 6 h reaction time.

Catalysts	$r_0 \times 10^5$ (mol/min g)	$r_{0/TA}$[a] (mol/min mmol NH_3)	Conversion (%)	Yield (%)
Zr-SBA15-08	9.23	8.23	64.3	63.1
WZSBA08-15-7	3.63	5.05	24.5	24.1
WZSBA08-15-8	6.88	4.81	54.6	53.8
WZSBA08-20-7	2.75	4.02	22.3	21.9
WZSBA08-20-8	6.40	6.40	38.2	37.9
Zr-SBA15-10	8.33	7.43	62.7	62.0
WZSBA10-15-7	3.88	5.44	23.9	23.6
WZSBA10-15-8	4.31	4.33	33.5	33.0
WZSBA10-20-7	3.46	5.10	22.5	22.1
WZSBA10-20-8	4.17	4.31	34.6	34.3

[a] $r_{0/TA}$ is defined as $r_0 \times 10^5$ per total acidity.

Table 4
Influence of temperature and feed composition on the initial rate of disappearance and conversion of cetyl alcohol and yield of cetyl palmitate over Zr-SBA15-08 catalyst after 6 h reaction time.

Temperature (°C)	CA/PA	$r_0 \times 10^5$ (mol/min g)	Conversion (%)	Yield (%)
135	1/1	4.94	42.6	41.1
162	1/1	9.23	64.3	63.1
162	1/2	13.00	83.8	83.3

Table 5
Influence of catalyst amount on the initial rate of disappearance and conversion of cetyl alcohol and yield of cetyl palmitate over Zr-SBA15-08 catalyst after 6 h reaction time.

Catalyst (%)[a]	$r_0 \times 10^5$ (mol/min)	Conversion (%)	Yield (%)
2.67	0.46	41.2	41.0
5.35	1.48	64.3	63.1
10.69	3.75	98.9	98.3

[a] Percentage of catalyst related to the total weight of reactants.

Table 6
Zr and W contents of fresh and used catalysts.

Catalysts	Zr content (wt%)		W content (wt%)	
	Fresh catalyst	Used catalyst	Fresh catalyst	Used catalyst
Zr-SBA15-08	7.91	7.52	–	–
WZSBA08-15-8	8.30	7.97	7.74	5.98
Zr-SBA15-10	8.03	7.92	–	–

cetyl palmitate yields as shown in Table 3. These catalysts had the highest total acidity and the highest amount of Brønsted acid sites. ZrSBA15-08 and Zr-SBA15-10 gave maximum conversions of 64.3 and 62.0%, respectively.

The catalyst activities were assessed by calculating initial disappearance rate of cetyl alcohol (r_o, mol/gcat min) and initial rate per acid site ($r_{0/TA}$, mol/mmol NH_3 min). They are tabulated in Table 3. The catalyst with high acidity gave high initial rate. Increasing Zr loading decreased initial rate. This was the result of the drop in the acidity of the catalyst observed. Loading tungsten further decreased initial rate of Zr-SBA-15 catalysts. Even more tungsten loading also reduced the initial rate. This was attributed to decrease in the acid sites as a result of WO_3 crystals formation which was discussed in the catalyst characterization section. However, rising calcination temperature from 700 to 800 °C, improved initial rate of reaction and cetyl alcohol yield. This was in line with the catalyst characterization results; as the higher calcination temperature enhanced acidity by decreasing WO_3 crystal size and providing the monolayer dispersion of WOx species which resulted in the improvement of the Brønsted acid sites.

Even though WZSBA08-15-8 catalyst had higher acidity than Zr-SBA15-08 and Zr-SBA15-10, it gave a lower initial rate per active site, $-r_{0/TA}$. This could be due to its lower Brønsted acid sites content, see B/L ratio given in Table 2. Therefore, it can be concluded that Brønsted acid sites were more effective for the reaction. The overall activities observed were found to be affected by catalyst deactivation behavior as well.

3.2.2. Influence of temperature

The reaction was also performed at 135 °C over Zr-SBA15-08 catalyst in order to investigate the influence of temperature. The initial activities, cetyl palmitate yield and conversion obtained are compared with these at 162 °C in Table 4. An increase of 27° in the reaction temperature produces almost two-fold increase in the initial disappearance rate of cetyl alcohol. Moreover, the conversion of cetyl alcohol and the yield of cetyl palmitate also increased by about 21%. These significant changes with temperature indicates that the reaction is kinetically controlled under conditions studied.

3.2.3. Influence of feed composition

From the economic point of the process, it is important to obtain high cetyl palmitate yield by using equimolar amounts of cetyl alco-

hol and palmitic acid. Since esterification is a reversible reaction, using an excess amount of one reactant shifts the reaction towards the products. The results of the catalytic tests using CA/PA ratio of 1/1 and 1/2 over Zr-SBA15-08 catalyst are given in Table 4. As expected, using an excess amount of palmitic acid increased both the initial disappearance rate of cetyl alcohol and the yield of cetyl palmitate substantially. Therefore, the process should be optimized by taking into account the yield of cetyl palmitate and the cost of excess reactants. Separation and recycling of excess reactant might be considered as a solution to achieve the optimum conditions.

3.2.4. Influence of catalyst amount

Catalyst amount was studied as another reaction parameter for the esterification of cetyl alcohol and palmitic acid. The catalytic tests were performed over Zr-SBA15-08 catalyst at 162 °C and the results are given in Table 5. The amount of catalyst raised the initial disappearance rate of cetyl alcohol and the yield of cetyl palmitate significantly. For example, conversion increased from 64.3 to 98.9% when a catalyst amount changed from 5.35% to 10.69%. An ester yield of 98% was obtained for 10.69% catalyst amount.

3.2.5. Catalyst stability and reusability

The reusability of the three most active catalysts (Zr-SBA15-08, Zr-SBA15-10 and WZSBA08-15-8) was tested up to three cycles. The results are given in Fig. 6. The activity of WZSBA08-15-8 catalysts decreased quite substantially in the second reuse. This could be due to the significant leaching of WO_3 species which was found from the results of XRF analysis given in Table 6. Although there was some Zr leaching, Zr-SBA15-08 catalyst showed no significant decrease in its activity up to 3rd reuse.
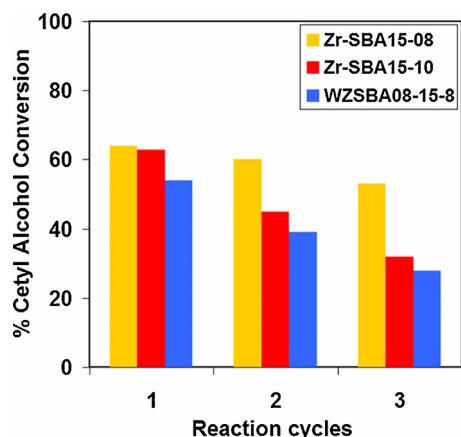
Fig. 6. Reusability of the catalysts.

4. Conclusions

Zr incorporated SBA-15 catalysts were found to be active, selective and reusable catalysts for esterification of palmitic acid and cetyl alcohol. Tungsten oxide loading on these Zr-SBA-15 catalysts decreased both the total acidity and the surface area of the catalyst resulting in the lower conversions of cetyl alcohol. The calcination temperature had an important effect on the structure and acidity of the catalysts. Higher calcination temperature favored the monolayer dispersion of WOx species leading to increase of Brønsted acid sites. The reaction tests were carried out under kinetically controlled condition. The higher cetyl alcohol conversions achieved with the catalysts calcined at a higher temperature are mainly due to the higher acidity of the catalysts. Reusability tests showed that Zr-SBA-15 catalysts retained its activity with reuse. The reaction was shifted to the product site with an increase in cetyl alcohol to a palmitic acid ratio which indicated that extent of the reaction was affected by the equilibrium.

Acknowledgments

References

[1] A.A. Costa, P.R.S. Braga, J.L. Macedo, J.A. Dias, S.C.L. Dias, Microporous Mesoporous Mater. 147 (2012) 142–148.
[2] J.M. Marchetti, A.M. Errazu, Fuel 87 (2008) 3477–3480.
[3] N. Özbay, N. Oktar, N.A. Tapan, Fuel 87 (2008) 1789–1798.
[4] M. Mazzotti, B. Neri, D. Gelosa, A. Kruglov, M. Morbidelli, Ind. Eng. Chem. Res. 36 (1997) 3–10.
[5] J.C. Juan, J. Zhang, M.A. Yarmo, Catal. Lett. 126 (2008) 319–324.
[6] J. Ni, F.C. Meunier, Appl. Catal. A 333 (2007) 122–130.
[7] S. Ramu, N. Lingaiah, B.L.A.P. Devi, R.B.N. Prasad, I. Suryanarayana, P.S.S. Prasad, Appl. Catal. A 276 (2004) 163–168.
[8] Y.M. Park, S.H. Chung, H.J. Eom, J.S. Lee, K.W. Lee, Bioresour. Technol. 101 (2010) 6589–6593.
[9] N. Laosiripojana, W. Kiatkittipongb, W. Sutthisripokc, S. Assabumrungrat, Bioresour. Technol. 101 (2010) 8416–8423.
[10] S. Patel, N. Purohit, A. Patel, J. Mol. Catal. A 192 (2003) 195–202.
[11] V. Brahmkhatri, A. Patel, Appl. Catal. A 403 (2011) 161–172.
[12] K. Mantri, R. Nakamura, Y. Miyata, K. Komura, Y. Sugi, Mater. Sci. Forum 539–543 (2007) 2317–2322.
[13] A. Sakthivel, K. Komura, Y. Sugi, Ind. Eng. Chem. Res. 47 (2008) 2538–2544.
[14] F.D. Gregorio, N. Keller, V. Keller, J. Catal. 156 (2008) 159–171.
[15] S. Kuba, P. Lukinskas, R.K. Grasselli, B.C. Gates, H. Knözinger, J. Catal. 216 (2003) 353–361.
[16] M.A.C. Jácome, C.A. Chavez, E.L. Salinas, J. Navarrete, P. Toribio, J.A. Toledo, Appl. Catal. A 318 (2007) 178–179.
[17] F. Figueras, J. Palomeque, S. Loridant, C. Fèche, N. Essayem, G. Gelbard, J. Catal. 226 (2004) 25–31.
[18] C. Zhang, T. Liu, H.J. Wang, F. Wang, X.Y. Pan, Chem. Eng. J. 174 (2011) 236–241.
[19] W. Sun, Z. Zhao, C. Guo, X. Ye, Y. Wu, Ind. Eng. Chem. Res. 39 (2000) 3717–3725.
[20] I.K. Mbaraka, D.R. Radu, V.S.Y. Lin, B.H. Shanks, J. Catal. 219 (2003) 329–336.
[21] I.K. Mbaraka, K.J. McGuire, B.H. Shanks, Ind. Eng. Chem. Res. 45 (2006) 3022–3028.
[22] E. Zhao, J. Feng, Q. Huo, N. Melosh, G.H. Fredrickson, B.F. Chmelka, G.D. Stucky, Science 279 (1998) 548–552.
[23] J.P. Thielemann, G. Weinberg, C. Hess, ChemCatChem 3 (2011) 1814–1821.
[24] Z.E. Berrichi, B. Louis, J.P. Tessonnier, O. Ersen, L. Cherif, M.J. Ledoux, C. Pahm-Huu, Appl. Catal. A 316 (2007) 219–225.
[25] C.W. Chiang, A. Wang, B.Z. Wan, C.Y. Mou, J. Phys. Chem. B 109 (2005) 18042–18047.
[26] J. Du, H. Xu, J. Shen, J. Huang, W. Shen, D. Zhao, Appl. Catal. A 296 (2005) 186–193.
[27] R. Grieken, J.M. Escola, J. Moreno, R. Rodríguez, Chem. Eng. J. 155 (2009) 442–450.
[28] S. Garg, K. Soni, G.M. Kumaran, M. Kumar, J.K. Gupta, L.D. Sharma, G.M. Dhar, Catal. Today 130 (2008) 302–308.
[29] P. Biswas, P. Narayanasarma, C.M. Kotikalapudi, A.J. Dalai, J. Adjaye, Ind. Eng. Chem. Res. 50 (2011) 7882–7895.
[30] M.D. Gracia, A.M. Balu, J.M. Campelo, R. Luque, J.M. Marinas, A.A. Romero, Appl. Catal. A 371 (2009) 85–91.
[31] Y.Q. Zhang, S.J. Wang, J.W. Wang, L.L. Lou, C. Zhang, S. Liu, Solid State Sci. 11 (2009) 1412–1418.
[32] N. Ieda, K. Mantri, Y. Miyata, A. Ozaki, K. Komura, Y. Sugi, Ind. Eng. Chem. Res. 47 (2008) 8631–8638.
[33] K. Mantri, K. Komura, Y. Sugi, Green Chem. 7 (2005) 677–682.
[34] S. Rajagopal, J.A. Martari, R. Miranda, J. Catal. 151 (1995) 192–203.
[35] A. Martinez, G. Prieto, M.A. Arribas, P. Concepcion, J.F.S. Royo, J. Catal. 248 (2007) 288–302.